THE EUROPEAN SOCIETY OF MEDICINE
Medical Research Archives, Volume 13 Issue 4

RESEARCH ARTICLE

Tomatidine Attenuates Inflammatory Responses to Exercise-Like Stimulation in Donor-derived Skeletal Muscle Myobundles

Maddalena Parafati[1]*, Tushar Sanjay Shenoy[1], Zon Thwin[1], Mauro Parlavecchio[2], Siobhan Malany[1]

[1]Department of Pharmacodynamics, College of Pharmacy, University of Florida, Florida 32610, USA.
[2]ArchiStudio, Orlando, Florida 32832, USA
*mparafati@ufl.edu

OPEN ACCESS

PUBLISHED
30 April 2025

CITATION
Parafati, M., et al., 2025. Tomatidine Attenuates Inflammatory and Functional responses to Exercise-Like Stimulation in Donor-derived Skeletal Muscle Myobundles. Medical Research Archives, [online] 13(4). https://doi.org/10.18103/mra.v13i4.6423

DOI
https://doi.org/10.18103/mra.v13i4.6423

ISSN
2375-1924

ABSTRACT

Donor-derived myotubes offer a pre-clinical model for studying muscle biology, the effects of exercise-like electrical stimulation, and assessing drug efficacy and toxicity. We engineered a 3D muscle microphysiological system from myoblasts isolated from vastus lateralis of young and older adults. Over a three-week differentiation process, we applied two cycles of low frequency electrical stimulation daily for seven days generating functional, mature myobundles, as confirmed by gene expression profiling. Both young- and old-derived myobundles showed synchronous contraction in response to electrical stimulation, however, the contraction magnitude was reduced in old-derived myobundles compared to young-derived myobundles. We then assessed the donor-specific response to tomatidine, a steroidal alkaloid found in the skin of green tomatoes, known to inhibit muscle atrophy and promote skeletal muscle hypertrophy. Bioinformatic analyses revealed that infusion of tomatidine during electrical stimulation modulated the IL-6/JAK/STAT3 pathway. The contraction magnitude decreased in the young-derived myobundles treated with tomatidine compared to vehicle-treated controls, while no significant difference was observed in the old-derived myobundles. Secretome analysis revealed age-related changes in secreted proteins linked to inflammation and extracellular matrix remodeling. Notably, tomatidine attenuates the inflammatory and extracellular matrix remodeling responses in the myobundles triggered by electrical stimulation, partially preventing the secretion of proinflammatory proteins. This intervention strategy helps balance muscle adaptation and repair, while limiting excessive proinflammatory responses. Our microphysiological system provides a valuable platform for investigating signaling pathways involved in muscle function, and pharmacological responses, advancing the understanding of age-related muscle biology.

Keywords: donor-derived myobundles; muscle-on-a-chip; E-Stim-induced contraction; transcriptome; secretome; inflammation; tomatidine.

Graphical abstract

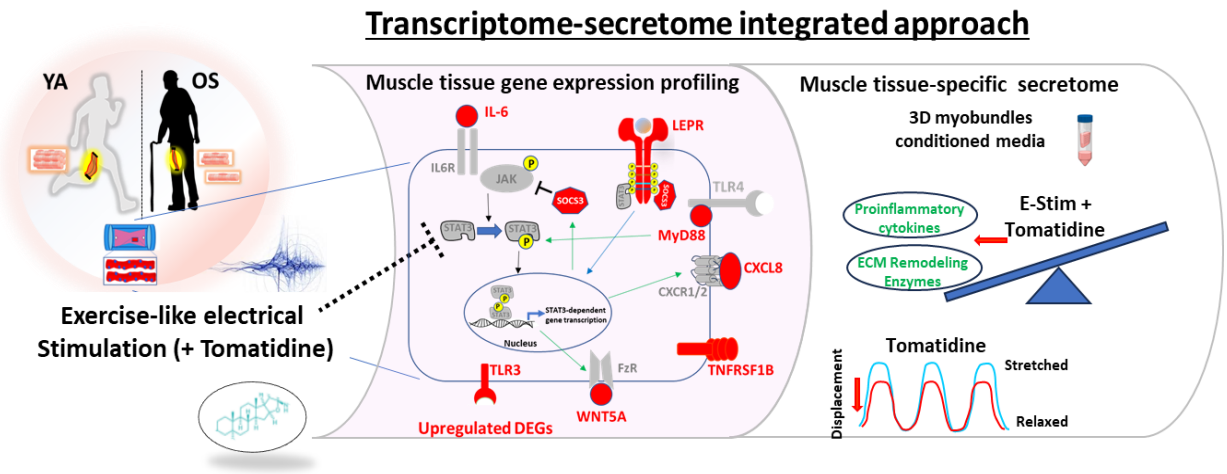

Introduction

The physiological effects of physical exercise are recognized for their beneficial impact on both the cardiovascular and musculoskeletal systems serving as preventive and therapeutic strategies for cardiovascular disease, diabetes, and obesity[1–4]. Repeated exercise induces an adaptive and transient response, including the release of cytokines, known as myokines[5], which play a critical role in the prevention and treatment of various chronic diseases[6,7]. Inflammation, often associated with tissue damage, is also a trigger of exercise-induced stress response, facilitating repair processes[8–10].

A critical process in skeletal muscle adaptation to exercise involves remodeling of the extracellular matrix (ECM), essential for effective muscle contraction, force transmission, and matrix reorganization[11–13]. Two enzymes families , matrix metalloproteinases (MMPs)[14] and tissue inhibitor of metalloproteinases (TIMPs)[15] are key regulators of ECM turnover. MMP-2 expression is decreased during low-intensity exercise[16] but increased in high-intensity exercise[17]. Among the four TIMP isoforms, TIMP-1 and -2 are significantly increased in response to exercise-like stimulation[18]. In parallel to ECM remodeling, myokines such as interleukin (IL)-6, IL-1β, IL-8, CC chemokine ligand 2 (CCL2) and tumor necrosis factor-alpha (TNF-α)[19] not only mediate inflammatory responses but also contribute to long-term adaptive responses to exercise training[20,21]. These cytokines also influence macrophages polarization towards a more pro-regenerative (M2) phenotype; thereby supporting muscle repair[22].

To better understand these processes, our microphysiological system (MPS) provides a valuable tool for modeling exercise regimens, evaluating proinflammatory markers and ECM remodelers and investigating mechanisms underlying muscle adaptation and atrophy. Advancements in 3D scaffold construction[25], and development of 3D microtissues able to self-organize following electrical stimulation (E-Stim)[26] have advanced tissue engineering field[27–29]. Our recent studies using donor-derived myobundles demonstrated a physiological response to daily electrical stimulation as evidenced by increased expression of myogenic genes, enhanced sarcomeric protein expression, and improved contractility, with distinct responsiveness observed between young- and old-derived myobundles[30,31]. Furthermore, prolonged electrical stimulation exposure has been shown to enhance myotube formation and accelerate differentiation rates in primary myoblasts culture[32–34]. In this study, we investigate the effects of electrical stimulation in the presence of nutritional supplement on muscle function.

Exercise and nutritional supplements maintain muscle mass throughout the life span[35,36]. Tomatidine, a steroid alkaloid found in green tomatoes, has been shown to inhibit age-related skeletal muscle atrophy[37]. This effect is mediated by the suppression

of activating transcription factor 4 (ATF4) expression, resulting in the attenuation of age-related decline in skeletal muscle strength, quality, and mass[38]. Tomatidine also demonstrates anti-inflammatory properties, including inhibiting LPS-stimulated murine macrophage via the suppression of NF-κB and JNK signaling pathways[39]. In vivo, tomatidine decreases inducible nitric oxide (iNOS), matrix metalloproteases, as well as other proinflammatory cytokines in a model of lung inflammation[40,41].

While tomatidine has shown promise in mitigating inflammation and muscle atrophy, its role in modulating cytokine secretion and ECM remodeling enzymes in response to electrical stimulation remains unexplored. Our study aims to address this gap by investigating anti-inflammatory effects of tomatidine on muscle contraction magnitude, ECM remodeling enzymes and cytokine secretion using phenotypic analysis, genome-wide transcriptomics, and quantitative secretome analysis, in young- and old-derived myobundles.

Tomatidine influenced contractility, particularly in young-myobundles, suggesting it may play a role in muscle cell homogeneity. The observed JAK/STAT3 modulation aligns with known pathways involved in muscle inflammation and repair, suggesting tomatidine's broader impact on exercise-induced signaling. Furthermore, we observed secreted pro-inflammatory cytokines IL-6, IL-6R, CXCL8/IL-8, CCL2, along with ECM turnover enzymes TIMP-1, and -2 throughout the electrical stimulation regime, which coincided with the differentiation of donor-derived myobundles. Notably, tomatidine treatment in electrically stimulated donor-derived myobundles involved the inhibition of pro-inflammatory cytokine secretion and ECM remodeling mediators. These insights provide critical evidence supporting tomatidine's protective effects during electrically stimulated muscle adaptation, laying the groundwork for future studies exploring combinatorial strategies involving bioengineered muscle models and nutritional interventions.

Methods

MUSCLE BIOPSY AND PARTICIPANTS CELL ISOLATION

Cell isolation was performed as previously described[42]. Briefly, vastus lateralis biopsies were obtained from young active (YA, age 21-40 years) and old sedentary (OS, age 65-80 years) volunteers, who gave written informed consent to participate in this study (n = 5), at the Translational Research Institute at AdventHealth (Orlando, Florida).

CELL CULTURE AND MYOBLAST IMMUNO-MAGNETIC CELL SORTING PROCEDURE

Myogenic precursors were thawed and then cultured on T150 flasks coated with collagen I (Rat Tail Collagen I, 0.1 mg/mL, ibidi) at density 2x 10^6 cells/ml and cultured in in Skeletal Muscle Growth medium (PromoCell, Heidelberg, Germany) for 3 days to reach confluency. The cell monolayer was rinsed with phosphate-buffered saline (PBS), treated with Accutase (StemCell) and purified by immuno-magnetic cell sorting (MACS) using CD56+ magnetic beads (Miltenyi Biotec) and mouse monoclonal 5.1 H11 anti-CD56 antibody (DSHB Hybridoma Bank, Iowa City, IA) to enrich for CD56 fractions as described[30]. CD56+ muscle myoblasts were expanded on T150 flasks coated with collagen I in Skeletal Muscle Growth medium to 70%, collected and cryopreserved.

MICTOFLUIDIC CHIP FABRICATION

Custom microfluidic chip design was performed by Micro-gRx, INC, (Orlando, FL). Devices were fabricated from polydimethylsiloxane (PDMS) and contained two platinum 22-gauge electrode leads as described[30,42]. Platinum electrodes are integrated into chips for electrical pulses stimulation and contractility real-time measurements. Before use, microfluidic chips were sterilized in ethanol and autoclaved at 150°C for 30 min prior to use with primary cell culture.

3D CELL CULTURE AND MYOTUBE DIFFERENTIATION

Microfluidic 3D cell culture was performed by combining thermosensitive hydrogel mixtures (3.3 mg/mL rat tail collagen I, and 22% (v/v) Matrigel) with CD56+ enriched myoblasts. The cell-laden hydrogels were injected into the PDMS chips to a final cell density of 15 and 20 million cells/mL for YA-and OS-derived cells, respectively as previously described[42]. Then, cell-encapsulated hydrogel was allowed to polymerize at 37°C for 60 min and seeding ports were sealed using polylactic acid plugs (PLA, Makerbot, Brooklyn, NY). To promote myoblast proliferation, tissue chips were perfused using a syringe pump for 2 days, through inlet and outlet ports of PDMS microfluidic channels with degassed Skeletal Muscle Growth medium (Promocell) supplemented with 0.1 mg/ml Primocin (InvivoGen, San Diego, CA), at a constant flow rate of 1 mL/h, at 37°C and 5% CO_2. Myoblasts were differentiated by a two-step process as described[30]. In brief, cells were perfused with stage 1 medium (MEM-α, 0.5% (v/v) ITS, 2% (v/v) B27, 10 μM DAPT, 1 μM Dabrafenib, 20 mM HEPES, pH 7.3 and, 0.1 mg/mL Primocin) at 125 mL/min every 6 h for 6 days followed by stage 2 maintenance medium (MEM-α, 0.5% (v/v) ITS, 2%(v/v) B27, 20 mM HEPES, pH 7.3 and, 0.1 mg/mL Primocin) at 125 mL/min every 6 h for an additional 6 days to promote maturation of myotubes.

ELECTRIC PULSE STIMULATION AND REAL-TIME RECORDING IMAGES ACQUISITION AND ANALYSIS

Differentiated myotubes were stimulated on day 14 with electrical pulses: 3 V/mm 2 ms and 2 Hz every 12 h for seven days[30]. On day 21, contractions were recorded at 10 fps for 40 s in an environmentally controlled Cytation C10 high content imager (Agilent, Biotek). Myotube contractility was quantified by digital image correlation (DIC). Reference images were taken before and during stimulation. 4x images are acquired with a resolution of 1224 × 904 pixels (12.5 x 143 mm). The region of interest (ROI) included the entire image excluding the micro post. DIC was performed using motion analyzer GOM correlate professional software (Zeiss, Germany) to determine displacement of the engineered myobundles. The reference image (the first frame prior to application of electrical stimulation) is compared to each test image (with E-Stim applied) in the sequence. After the analysis, the DIC values are saved as a raw EXCEL file that stores the numerical displacement info for each grid at individual frames. Each frame represents a timepoint and subsequent frames are plotted as time on the X-axis. The average pixel value across the rows and columns in the ROI is converted to microns (1.75 μm/pixel) and plotted on the Y-axis as displacement to generate a graph of displacement vs. time.

TOTAL RNA EXTRACTION AND RNA SEQUENCING ANALYSIS

Total cellular RNAs were isolated from myobundles using RNeasy kits, as described by the manufacturer (Qiagen). Total RNA was subjected to DNase Digestion (Qiagen). In addition to concentration and purity, we determined the quality of RNA samples (**Table 1**) prior to library preparation for RNA-Seq as described[42]. Briefly, the purity and quality of both extracted RNA samples were assessed by spectrophotometry (NanoDrop; Thermo Scientific) (A260/A280) and their integrity using Agilent 2200 Tapestation system (Agilent, Santa Clara, CA) respectively. 500 ng of total RNA was used for RNA-Seq. Libraries of extracted RNA samples were built using the NEBNext® Ultra™ Directional RNA Library Prep Kit for Illumina (NEB, USA) RNA sample preparation kit and yielded fragments with 220–700 base pairs. The qualified fragments were ligated with 60 adapters, amplified, and submitted for sequencing by Illumina NovaSeq 6000 (Illumina, San Diego, CA) to generate paired end reads with a length of 150 bases. The input sequences were trimmed using trimmomatic. Quality control was performed before and after trimming using FastQC (v 0.11.4) and MultiQC and a total of 50 million reads were generated for each sample yielding coverage in the range of 118 to 220 bases for each sample, Input sequences were aligned to the transcriptome using the STAR aligner, version 2.7.9a.

Transcript abundance was quantified using RSEM (RSEM v1.3.1), and genes with insufficient average counts were excluded from further statistical analysis. Differential expression analysis was performed using the DESeq2 package, with an FDR-corrected P-value threshold of 0.05. The results were further filtered to extract transcripts showing a 2.0-fold change (log_2FC) in either direction.

Table 1. RIN analysis

Groups	Sample #	Cohort	Description	RNA(ng)	RIN
Differentiated myobundles					
1	1	Young E-Stim	Vehicle (Ctrl)	2741.5	9
	2	Young E-Stim	Vehicle (Ctrl)	1766.3	8.4
	3	Young E-Stim	Vehicle (Ctrl)	1626.3	8.9
2	4	Old E-Stim	Vehicle (Ctrl)	1793.4	8.7
	5	Old E-Stim	Vehicle (Ctrl)	2072.7	8.6
	6	Old E-Stim	Vehicle (Ctrl)	2200.3	7.6
3	7	Young E-Stim	Tomatidine	1989.1	9.8
	8	Young E-Stim	Tomatidine	2184.1	9.1
	9	Young E-Stim	Tomatidine	2002.3	9.2
4	10	Old E-Stim	Tomatidine	2088.5	9.2
	11	Old E-Stim	Tomatidine	2365.4	9.5
	12	Old E-Stim	Tomatidine	2087.4	9.1

DIFFERENTIAL EXPRESSION AND FUNCTIONAL ANNOTATION ANALYSIS OF RNA-seq DATA

Differentially expressed genes (DEGs) from tomatidine-treated YA- and OS-derived myobundles were normalized to the matching control group and reported as log_2 of the fold change (log_2FC). Fold induction values were averaged for all experiments performed as experimental triplicates for each cohort. Volcano plots, which rely on double filtering criterion and display unstandardized signal log_2FC against noise-adjusted/standardized signal FDR-corrected *P*-value, were used to display up- and down-regulated DEGs. Database for Annotation, Visualization, and Integrated Discovery database (DAVID, https://david.ncifcrf.gov/) was used to determine the biological meaning to a given set of DEGs and categorized them by Gene Ontology (GO)-molecular function, GO-biological process, and GO-cellular component as previously described[42]. In DAVID database, Fisher's Exact test is adopted to measure gene-enrichment in annotation terms. Fisher's Exact *p*-values are computed by summing probabilities p over defined sets of tables ($Prob=\sum Ap$) compared against a background that consists of all *Homo Sapiens* genes. The number of DEGs annotated to the term is compared against the number of genes expected by chance. Significance of each GO term was assessed using the default *homo sapiens* GO annotation as background. A GO term was considered statistically significant at FDR-corrected $P \leq 0.05$. For further interpretation of gene expression data and pathway analysis, gene set enrichment analysis (GSEA) on the KEGG pathways was performed by using GSEA software, an integrative web-based software application, using pathway definitions from Molecular Signatures Database (MSigDB), developed by Broad Institute[43].

COLLECTION OF CONDITIONED MEDIA AND HUMAN INFLAMMATORY CYTOKINE AND ECM ARRAYS

Myobundles were perfused with vehicle (EtOH, %) and tomatidine (5 uM) simultaneously with the onset of electrical stimulation (E-Stim) and continued for 7 days. At the conclusion of E-Stim, serum-free conditioned media were collected, centrifuged at 3000 rpm for 20 min at 4°C in presence of 10 µg/ml phosphatase inhibitor cocktail (Thermo Fisher Scientific) and 10 µg/ml protease inhibitor cocktail (Sigma) and stored at -80°C until use. The human inflammatory antibody array including 40 proteins (AAH-INF-3, RayBioTech, Norcross, GA) was used

to screen for pro-inflammatory cytokines and ECM enzymes (AAH-MMP-1-2, RayBioTech, Norcross, GA) as per manufacturer's instructions. 1.5 mL culture supernatant was concentrated to 800 µL using protein concentrators with a molecular weight 3 kDa cut-off (ThermoFisher scientific). Briefly, the membranes were blocked for 30 min at room temperature (RT) and then incubated overnight (O/N) at 4°C with concentrated conditioned raw media. Subsequently, the membranes were washed 3x with wash buffer I and 2x with wash buffer II. The washed membranes were then loaded with biotinylated cocktail and incubated for 2h at RT followed by subsequent wash steps and loaded with horseradish peroxidase (HRP)–streptavidin cocktail for 2 h at RT. Following further washing, chemiluminescence detection solution was applied for 2 min and specific protein signal was detected using the ChemiDoc™ Touch Imaging System (BioRad). The individual spots were quantified using imageJ software (https://imagej.net/ij/) and the spots representing specific proteins were normalized to positive controls included in the array, yielding a relative density for each spot and expressed as relative quantity.

DATA AVAILABILITY

All data generated during this study are either included in the manuscript or are available at the Gene Expression Omnibus (GEO) database (GSE296683). Precursor cells from patient biopsy samples were obtained from AdventHealth Orlando through a Material Transfer Agreement to the University of Florida with restrictions for sharing with a third party.

Results

TOMATIDINE TREATMENT MODULATES CONTRACTILE FUNCTION IN DONOR-DERIVED MYOBUNDLES

We previously demonstrated induced muscle contraction in tissue-engineered human skeletal myobundles through electrical stimulation (E-Stim)[30,42]. In this study, we applied a similar electrical stimulation regime. On day 14, differentiated myotubes, under mechanical tension, were exposed to two 30-min E-Stim cycles per day followed by a 12 h recovery period. The stimulation protocol was continued for seven days, and by day 21, the donor-derived myobundles displayed highly aligned myotubes oriented along the direction of the applied electric field[31]. Prior to nucleic acids extraction, myotubes underwent a final round of electrical stimulation, and contractile movement was recorded by confocal imaging. Using digital image correlation (DIC) analysis, we observed a significant increase in contractility magnitude and synchronicity of vehicle-treated donor-derived myobundles compared to previous 5-day E-Stim regime[30] (**Figure 1A**).

Specifically, young active (YA)-derived myobundles showed average contraction displacement of 15 ± 2.8 µm, while old sedentary (OS)-derived myobundles exhibited an average displacement of 8.7 ± 0.9 µm (**Figure 1B**). In the absence of electrical stimulation, the myotube displacements in both YA and OS groups were comparable to baseline measured during the resting phase. When tomatidine (5 µM), was administered every 6 h for seven days during E-Stim, a significant reduction in contraction displacement (10.5 ± 1.3 µm) was observed in the younger cohort. In contrast, the older cohort did not show a significant difference in contraction compared to vehicle treated (7.8 ± 0.6 µm) (**Figure 1B**). Our data show that muscle twitch kinetics are age-dependent. Tomatidine exposure is associated with reduced variability in both cohorts.

TOMATIDINE INCREASED GENES ASSOCIATED WITH IL-6/JAK-STAT SIGNALING PATHWAY IN YOUNG E-STIM MYOBUNDLES

Tomatidine has been shown to exhibit protective effects against the release of pro-inflammatory cytokines/chemokines[5] and to mitigate skeletal muscle atrophy both in vivo and in vitro[37]. In our study, treatment of YA-derived E-Stim myotubes revealed 215 increased and 219 decreased DEGs compared to E-Stim matched control (**Figure 2A**). In contrast, treatment in OS-derived myobundles induced a significantly smaller number of DEGs, with only 12 increased and 2 decreased DEGs compared

to ground controls (Figure 2B). GSEA analysis based on the Kyoto Encyclopedia of Genes and Genomes (KEGG) pathway database highlighted a significant enrichment of DEGs involved in responses to tomatidine, particularly those associated with the activation of Janus kinase (JAK)/signal transducer and activator of transcription (STAT) signaling pathway (Figure 2C).

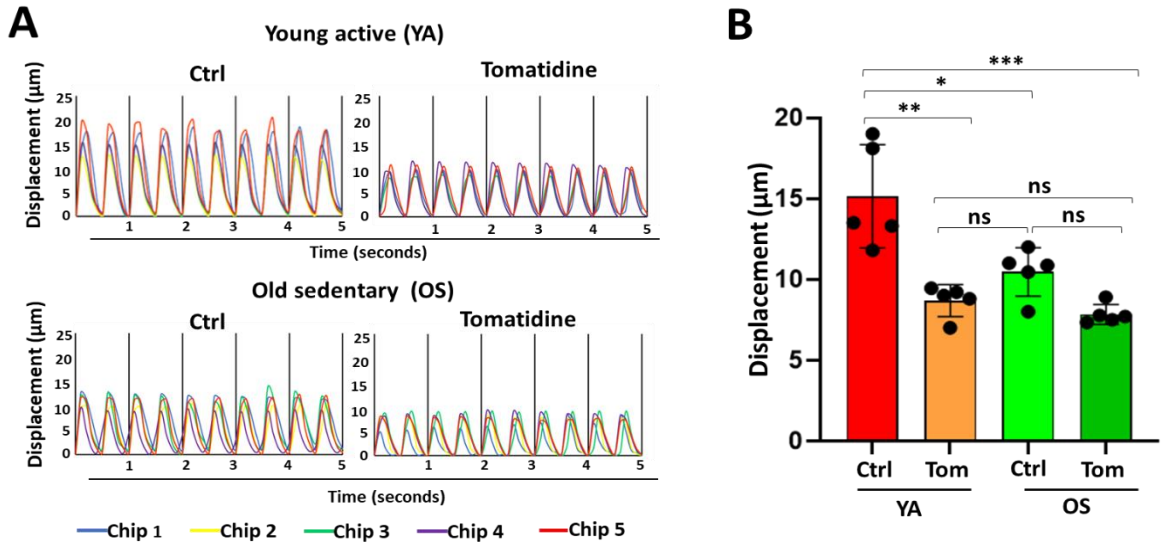

Figure 1. Functional analysis of 3D donor-derived myobundles. A. Donor-derived human myobundles electrically stimulated (E-Stim, 3 V, 2 Hz, 2 ms) for 7 days twice a day. B. Displacement measurements were quantified using DIC algorithm at day 21 across groups. Bar graph indicates displacement values (µm) in myobundles during E-Stim in the absence and presence of tomatidine (n=5). Data are presented as mean ± SD. Statistical significance determined by one-way ANOVA followed by Tukey's post-test correction was applied. * $p \leq 0.0053$, ** $p \leq 0.0003$, *** $p \leq 0.0001$.

The JAK/STAT signaling pathway is a critical mediator that transmits extracellular signals to the nucleus, initiating the transcription of genes involved in several biological activities. In skeletal muscle, this pathway plays a central role in regulating skeletal muscle mass, repair, and the pathogenesis of muscle-related diseases. Activation of the JAK/STAT pathway can yield opposite effects on muscle differentiation and repair[44]. In our study, we observed upregulation of several STAT3 gene targets, including the leptin receptor (LEPR) (1.2-fold increase), Wnt family member 5A (WNT5A) (0.9-fold increase), Toll-like receptor 3 (TLR3) (1.6-fold increase), and tumor necrosis factor receptor superfamily member 1B (TNFRSF1B) (2.3-fold increase). In addition, the suppressor of cytokine signaling (SOCS) 3 (1.3-fold increase), an inducible negative feedback inhibitor of cytokine signaling, was also upregulated. These results are consistent with an overall increase in STAT3 target genes, which also included a modest upregulation of myeloid differentiation primary response 88 (MyD88) (0.6-fold increase). MyD88 plays a key role in promoting skeletal muscle growth in vivo[45] and mediating STAT3 phosphorylation[46].

A marked 5-fold increase in IL-6 and 1.6-fold increase in IL-8/CXCL8 mRNA expression was observed in YA -derived samples following exercise-like electrical stimulation in the presence of tomatidine. Although there was a trend toward increased expression of genes downstream of STAT3 signaling in YA-derived myobundles, none of the changes reached statistical significance compared to OS-derived myobundles treated with tomatidine (Figure 2B). Among the increased DEGs, we identified genes encoding proteins involved in cell differentiation and protein-protein interactions, including MEF2B, CDC20, SRD5A1, TNXB, WDR78, ADGRB1, FAM83D, TNFRSF1B, ESCO2, TGFBR3. We observed a 1.9-fold increase in myocyte enhancer factor 2 B (MEF2B) and a 6.5-fold increase in adhesion G protein-coupled receptor B1 (ADGRB1). Both genes are crucial for modulating proper muscle cell signaling pathways and promoting muscle

regeneration (**Figure 2D**). Our results highlight an important role of tomatidine in modulating IL-6/JAK/STAT3 proinflammatory signaling during E-Stim-induced contraction.

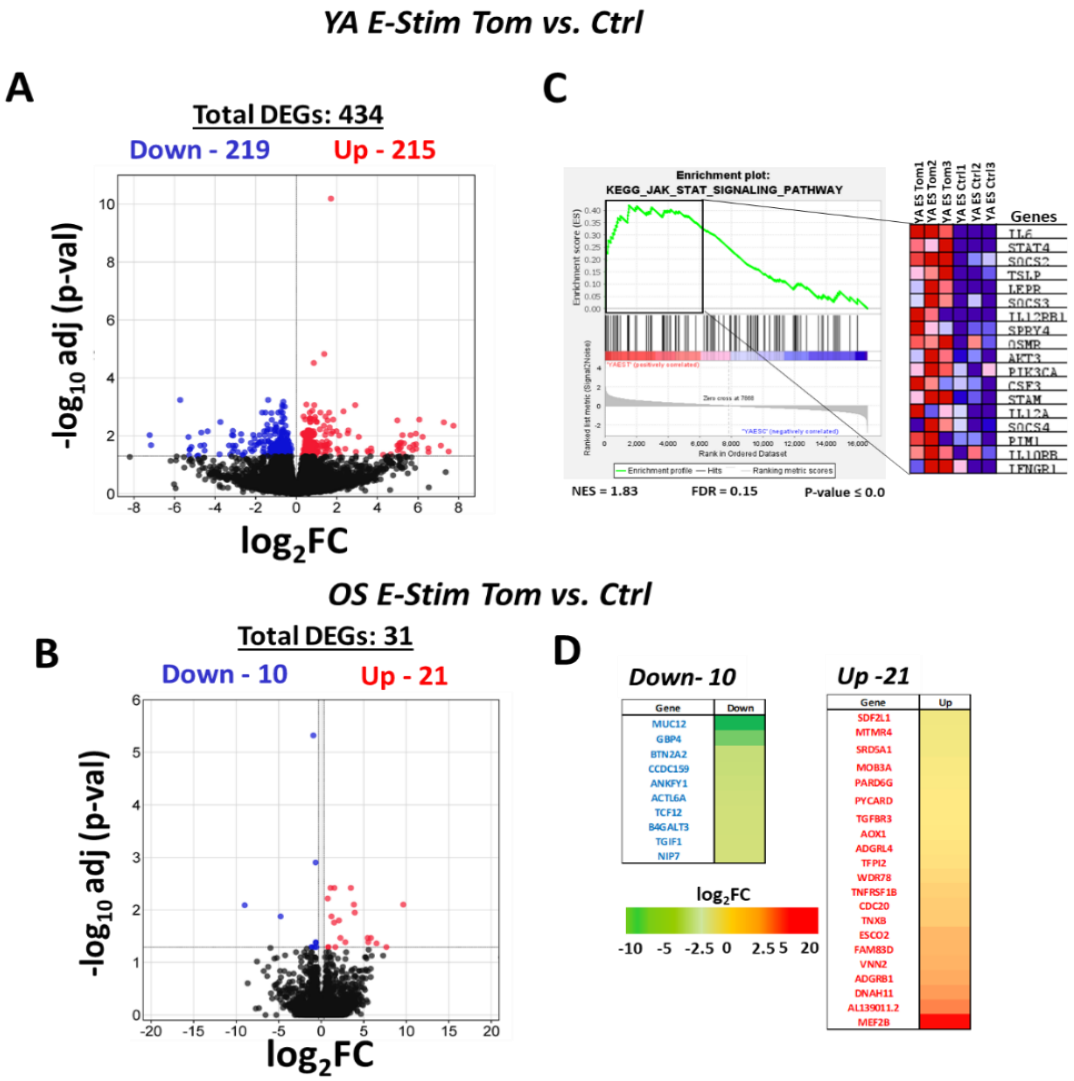

Figure 2. Visualization of RNA-Seq results and functional enrichment analysis of DEGs. **A, B**. Volcano plots of log2 fold change (log2FC) versus –log10 FDR of the differentially regulated genes (DEGs). Red and blue circles indicated up- and down-regulation of DEGs respectively; black circles denoted non-DEGs. **C.** KEGG pathway enrichment analysis using Gene set enrichment analysis (GSEA). **D**. Heatmaps of the down- and up-regulated DEGs between old (OS) tomatidine-treated vs. control group. Data are representative of three independent tissue chip RNA-seq determinations.

E-STIM-INDUCED CONTRACTION DRIVES MYOKINES SECRETION, WHILE TOMATIDINE INHIBITS THEIR RELEASE

Although we identified activation IL-6/JAK/STAT3 signaling pathway, the underlying mechanism remained unclear. Therefore, we aimed to further investigate the role of IL-6/JAK/STAT3 signaling pathway in inflammation. To validate pathway activation, donor-derived myobundles were analyzed post E-Stim using inflammatory cytokine and ECM antibody arrays (**Figure 3**) to quantify up to 40 cytokines and 10 ECM remodel enzymes, respectively, secreted into the conditioned media of donor-derived myobundles after the final E-Stim cycle.

Despite a marked increase in IL-6 mRNA, the corresponding IL-6 protein levels in the conditioned media remained detectable but were not elevated (**Figure 3B-G**). A soluble form of the IL-6 receptor was also secreted by the donor-derived myobundles.

Additionally, we found marked increases in two chemokines, monocyte chemoattractant protein-1 (MCP-1/CCL2) and IL-8/CXCL8, in the secretome of both YA- and OS-derived contracting myobundle (**Figure 3B-G**). In particular, we observed similar levels of IL-8 and increased CCL2 by 1.6-fold in YA-derived myobundles when compared to the old. Consistent with the mechanical changes associated with E-Stim-induced exercise and myogenesis, both contracting myobundles exhibited in the conditioned media the presence of tissue inhibitor of metalloproteinases 1 and 2 (TIMP-1, -2) (**Figure 3D-G**). The analysis showed a 2- and 1.3-fold increase in TIMP-1 and TIMP-2 protein secretion, respectively, by OS-derived myobundles when compared with the young in the control conditions. Interestingly, the current results show that the expressions of pro-enzymes and activated forms of MMPs-(1, 2, 3, 8, 9, 10 and 13) were not detectable by the array antibodies (**Figure 3F-G**).

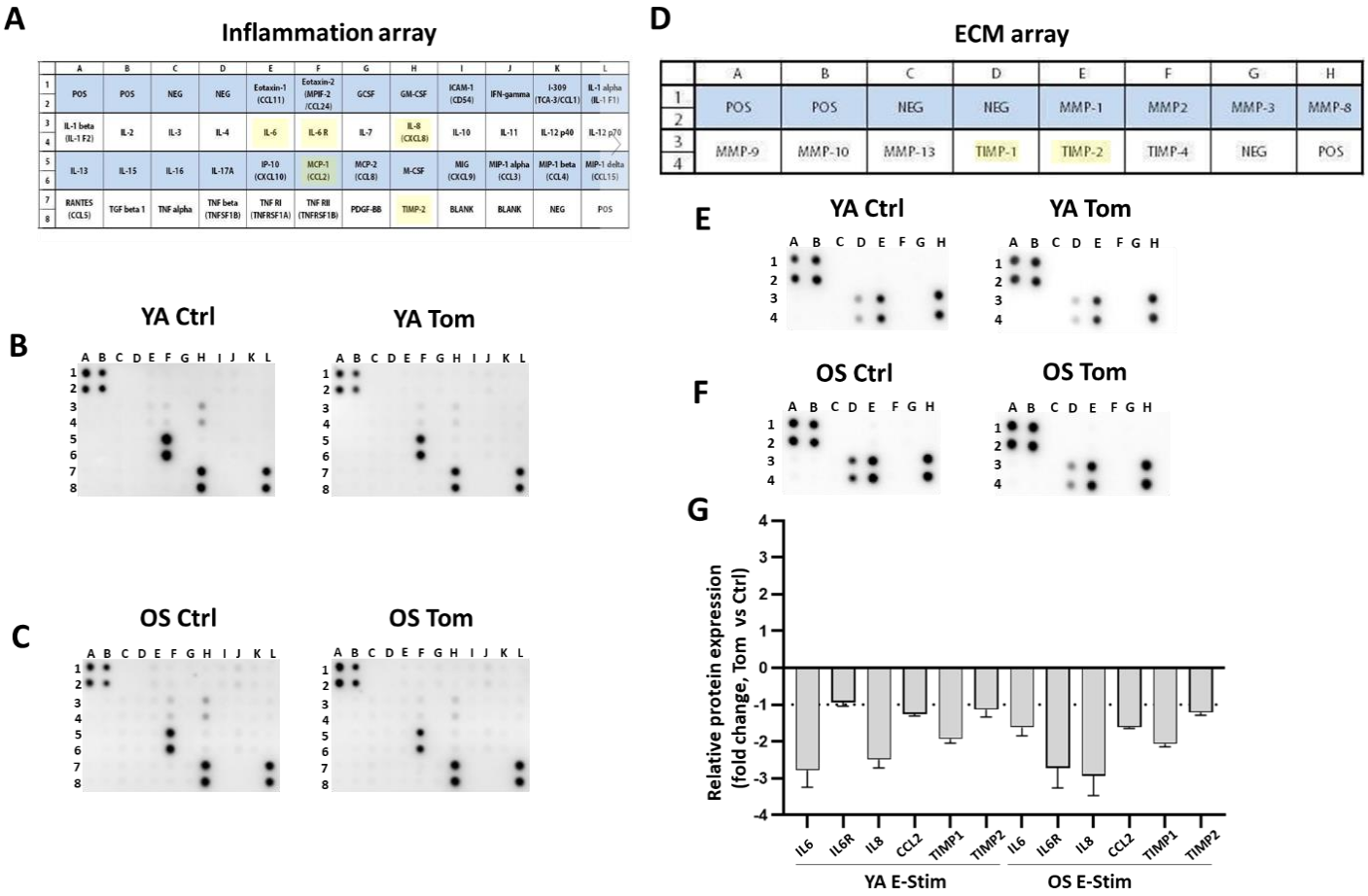

Figure 3. Comparison between secretomes of electrically stimulated donor-derived myobundles. **A.** Layout of the human inflammation array. **B, C.** Human muscle array readouts of inflammation secreted proteins. **D.** Layout of the human extracellular matrix (ECM) array. **E, F.** Human muscle array readouts of ECM secreted proteins. **G.** Normalized intensity expressed as fold change of the arrays (**B, C,** E and F). The individual spots were normalized to positive controls. Fold changes given as mean ± SD from 3 pooled independent experiments is shown.

Studies have highlighted the anti-atrophic properties of tomatidine in muscle (Ebert et al., 2019). However, its age-related anti-inflammatory effect in bioengineered skeletal muscle models and the underlying mechanism has not been previously explored. We administered tomatidine intermittently every six hours for seven days in donor-derived myobundles during low-frequency E-Stim induced contraction. Consistent with the natural products' anti-inflammatory properties, tomatidine treatment led to decreased IL-6 secretion of 2.7-fold in YA- and 1.6-fold in OS-derived myobundles, as well as a 2.7-fold reduction in the secretion of its receptor in OS-derived myobundles (**Figure 3G**). Furthermore,

tomatidine inhibited the secretion of IL-8/CXCL8, with a greater reduction of 2.5-fold in the YA group compared to a 2.9-fold reduction in the OS group (**Figure 3G**). MCP-1/CCL2 secretion was reduced by 1.2- and 1.6-fold in YA- and OS-derived myobundles, respectively, following tomatidine treatment. Lastly, whereas TIMP-2 levels were not altered in both groups by tomatidine, we observed a decrease by 1.9- and 2-fold for TIMP-1 in YA- and OS-derived myobundles, respectively (**Figure 3G**).

Discussion

Understanding muscle cell-autonomous mechanisms underlying age-related muscle inflammation following exercise is critical to prevent muscle injury, chronic inflammation, attenuating inflammatory responses that disrupt muscle regeneration and adaptive remodeling[47]. Compared to traditional 2D models, 3D bioengineered skeletal muscle derived from cultured myotubes offer significant advancement in modeling exercise in vitro[48,49] while also preserving phenotypical characteristics, as primary cells maintain the genetic[30] and the epigenetic background of the donor[49]. Myoblasts embedded in a 3D matrix allow for extended culture time, myotubes maturation and enhanced contractility[31]. In this study, we used 3D donor-derived engineered myobundles to model inflammation-induced adaptation during low-frequency intermittent E-Stim- and to investigate the anti-inflammatory effects of tomatidine on muscle function, comprehensive gene signatures by RNA-sequencing, and the secretome.

Previously, we demonstrated that donor-derived myobundles exhibited hallmarks of muscle aging, providing an in vitro platform to study structural and genetic changes as well as contractile responses of YA- and OS-derived skeletal muscle to exercise-like E-Stim[30]. E-Stim is well established for inducing myogenic differentiation and myobundle hypertrophy[23,30] and is used to examine exercise effects on muscle cell biology and function. We showed that a 7-day E-Stim regime resulted in synchronized, age-dependent increases in contraction displacement between YA- and OS-derived myobundles[30,31]. E-Stim significantly increased skeletal muscle-specific structural proteins and pro-myogenic transcription factors involved in muscle differentiation[31]. Additionally, we revealed muscle-autonomous activation of IL-6/JAK/STAT3 signaling, a key mediator of adaptive remodeling during E-Stim.

Exercise-induced regenerative inflammation[50] promotes tissue repair[47]. Skeletal muscle functions as a secretory organ, releasing bioactive molecules such as myokines and extracellular vesicles-derived factors, to modulate immune responses. Exercise alters cytokine secretion, promoting muscle repair[51], reducing inflammation[52–54] preventing atrophy and promoting neo-angiogenesis[55,56]. Muscle fiber's anti-inflammatory effects are largely attributed to the release of signaling molecules that modulate proinflammatory non-muscle cells, thereby reducing inflammation[57]. In this study, we examined the muscle cell-autonomous mechanisms of age-related inflammation in 3D donor-derived engineered myobundles. Our results indicate that E-Stim induced secretion of cytokines, chemokines, and ECM remodeling enzymes, including contraction-regulated myokines such as IL-6, IL-8, CCL2[57,58], as well as ECM-related proteins TIMP-1 and TIMP-2[59]. However, prolonged inflammatory responses can impair repair mechanisms, leading to fibrosis[60,61]. The JAK/STAT, associated to low-grade inflammation, has been linked to muscle wasting[62].

Our results are consistent with studies showing that blocking STAT3 can suppress the expression of caspase-3, MAFbx, and myostatin, thus alleviating skeletal muscle wasting in cancer cachexia[63] and rescues denervation-induced skeletal muscle atrophy[64]. Inhibition of the JAK/STAT pathways in aged mice alleviates pro-inflammatory senescence-associated secretory phenotype (SASP) in adipose tissue[65] and enhances skeletal muscle function in 3D constructs[66]. We demonstrated that tomatidine, known for its anti-trophic properties[37], mitigated exercise-like stimulation-induced inflammation by reducing IL-6, IL-8, CCL2 and TIMP-1 secretion in both

YA- and OS-derived myobundles, helping balance inflammatory responses and muscle adaptation.

We propose that tomatidine may inhibit IL-6 and IL-8 translation or secretion and their receptor expression during E-Stim. This likely reflects the acute IL-6 and IL-8 release and STAT3 activation commonly associated with atrophy in conditions such as obesity, diabetes, sarcopenia, or cancer[67]. Secreted TIMPs inhibit the activity of multiple metalloproteases (MMPs)[68] by forming non-covalent complexes preventing ECM degradation. Interestingly, MMPs-(1, 2, 3, 8, 9, 10 and 13) were undetectable in conditioned media of both donor-derived myobundles. This may be due to our sample preparation method not dissociating MMP-TIMP complexes altering the structure recognized by the antibodies. Our findings establish donor-derived myobundles as a physiologically relevant model for investigating skeletal muscle adaptation to exercise and ECM remodeling. Moreover, we highlight the role of tomatidine in modulating IL-6/JAK/STAT3 signaling pathway during E-Stim-induced contraction.

Conclusions

In conclusion, we demonstrate that our muscle MPS serves as a valuable age-related translational model for mimicking age-related muscle inflammation following exercise-like E-Stim. Physical exercise triggers the release of a cascade of cytokines, including tumour necrosis factor (TNF)-α, interleukin (IL)-1β, IL-6, IL-1 receptor antagonist, TNF receptors, IL-10 and IL-8, which function as autocrine and/or paracrine mediators[21,69–71]. Several studies have indicated that the JAK/STAT3 signaling pathway is activated in response to muscle contractions, exercise induced muscle damage and inflammation. However, it remains unclear whether activation of this pathway can contribute to local inflammation and ECM remodeling and promote muscle regeneration. For example, resistance exercise activates the IL-6/STAT1/STAT3 signaling pathway in rat skeletal muscle[72] and in human muscle[73], suggesting a potential role for STAT3 in the adaptive growth of skeletal muscle mediated by adult satellite cells. Additionally, we showed the specific effects of tomatidine on muscle contractility in donor-derived myobundles. We also demonstrated an anti-inflammatory mechanism during muscle exercise adaptation involving potential crosstalk with IL-6/JAK/STAT3 pathway. When tightly regulated, this pathway may protect against inflammation and contribute to the improvement of skeletal muscle repair and remodeling following exercise.

Author contributions:

Conceptualization, M.P. and S.M.; Investigation and methodology, M.P. and S.M.; Isolation and amplification of CD56+ human myoblasts, M.P, S.T. & Z.T; Cell seeding and culturing experiments, M.P.; Bioinformatic and antibody arrays analysis: M.P.; Digital image correlation analysis, M.Parla; Project administration, S.M.; Providing reagents and materials, S.M.; Writing - original draft and preparing all figures, M.P.; Writing - review & editing, M.P. & S.M.; Funding acquisition, S.M.; Overall project supervision, M.P. & S.M.; All authors have read and agreed to the published version of the manuscript.

Conflicts of Interest Statement:

S. Malany is a member of the board at Micro-gRx, INC. All other authors declare they have no conflicts of interest with the contents of this article.

Funding Statement:

This study was supported by the National Institutes of Health National Center for Advancement of Translational Sciences (5UG3TR002598 to S.M.) and the Center for the Advancement of Science in Space (CASIS) user agreement #UA-2019-011 to the University of Florida and University of Florida Prosper Bridge Fund (M.P.).

Acknowledgments:

The Authors thank the scientific program manager Dr. Lucie Low for advocating the NIH Tissue Chips program at the National Center for Advancing Translational Sciences (NCATS). We thank Austin Hinkle for helping with creating microfluidic devices as an intern at Micro-gRx. We thank the Interdisciplinary

Center for Biotechnology Research (ICBR) at the University of Florida NextGen Sequencing Core (RRID:SCR_019152) and Alberto Riva at UF|ICBR Bioinformatics Core.

References:

1. Gronek, P. *et al.* A Review of Exercise as Medicine in Cardiovascular Disease: Pathology and Mechanism. *Aging and disease* **11**, 327 (2020).

2. Izquierdo, M. *et al.* International Exercise Recommendations in Older Adults (ICFSR): Expert Consensus Guidelines. *The Journal of nutrition, health and aging* **25**, 824–853 (2021).

3. Syeda, U. S. A., Battillo, D., Visaria, A. & Malin, S. K. The importance of exercise for glycemic control in type 2 diabetes. *American Journal of Medicine Open* **9**, 100031 (2023).

4. Chomiuk, T., Niezgoda, N., Mamcarz, A. & Śliż, D. Physical activity in metabolic syndrome. *Front. Physiol.* **15**, 1365761 (2024).

5. Lee, J. H. & Jun, H.-S. Role of Myokines in Regulating Skeletal Muscle Mass and Function. *Front. Physiol.* **10**, 42 (2019).

6. Mathur, N. & Pedersen, B. K. Exercise as a Mean to Control Low-Grade Systemic Inflammation. *Mediators of Inflammation* **2008**, 109502 (2008).

7. Severinsen, M. C. K. & Pedersen, B. K. Muscle–Organ Crosstalk: The Emerging Roles of Myokines. *Endocrine Reviews* **41**, 594–609 (2020).

8. Suzuki, K. Cytokine Response to Exercise and Its Modulation. *Antioxidants* **7**, 17 (2018).

9. Oishi, Y. & Manabe, I. Macrophages in inflammation, repair and regeneration. *International Immunology* **30**, 511–528 (2018).

10. Cerqueira, É., Marinho, D. A., Neiva, H. P. & Lourenço, O. Inflammatory Effects of High and Moderate Intensity Exercise—A Systematic Review. *Front. Physiol.* **10**, 1550 (2020).

11. Jiao, A. *et al.* Regulation of skeletal myotube formation and alignment by nanotopographically controlled cell-secreted extracellular matrix. *J Biomedical Materials Res* **106**, 1543–1551 (2018).

12. Osses, N., Casar, J. C. & Brandan, E. Inhibition of extracellular matrix assembly induces the expression of osteogenic markers in skeletal muscle cells by a BMP-2 independent mechanism. *BMC Cell Biol* **10**, 73 (2009).

13. Melo, F., Carey, D. J. & Brandan, E. Extracellular matrix is required for skeletal muscle differentiation but not myogenin expression. *J. Cell. Biochem.* **62**, 227–239 (1996).

14. Mu, X., Urso, M. L., Murray, K., Fu, F. & Li, Y. Relaxin Regulates MMP Expression and Promotes Satellite Cell Mobilization During Muscle Healing in Both Young and Aged Mice. *The American Journal of Pathology* **177**, 2399–2410 (2010).

15. Alameddine, H. S. Matrix metalloproteinases in skeletal muscles: Friends or foes? *Neurobiology of Disease* **48**, 508–518 (2012).

16. Carmeli, E., Moas, M., Lennon, S. & Powers, S. K. High intensity exercise increases expression of matrix metalloproteinases in fast skeletal muscle fibres. *Experimental Physiology* **90**, 613–619 (2005).

17. Mackey, A. L., Donnelly, A. E., Turpeenniemi-Hujanen, T. & Roper, H. P. Skeletal muscle collagen content in humans after high-force eccentric contractions. *Journal of Applied Physiology* **97**, 197–203 (2004).

18. Heinemeier, K. M. *et al.* Expression of collagen and related growth factors in rat tendon and skeletal muscle in response to specific contraction types. *The Journal of Physiology* **582**, 1303–1316 (2007).

19. Tuttle, C. S. L., Thang, L. A. N. & Maier, A. B. Markers of inflammation and their association with muscle strength and mass: A systematic review and meta-analysis. *Ageing Research Reviews* **64**, 101185 (2020).

20. Bettariga, F. *et al.* Exercise training mode effects on myokine expression in healthy adults: A systematic review with meta-analysis. *Journal of Sport and Health Science* **13**, 764–779 (2024).

21. Pedersen, B. K., Åkerström, T. C. A., Nielsen, A. R. & Fischer, C. P. Role of myokines in exercise and metabolism. *Journal of Applied Physiology* **103**, 1093–1098 (2007).

22. Lesnak, J. B., Berardi, G. & Sluka, K. A. Influence of routine exercise on the peripheral immune system to prevent and alleviate pain. *Neurobiology of Pain* **13**, 100126 (2023).

23. Khodabukus, A. *et al.* Electrical stimulation increases hypertrophy and metabolic flux in tissue-engineered human skeletal muscle. *Biomaterials* **198**, 259–269 (2019).

24. Kim, J.-H., Yu, S.-M. & Son, J. W. Human Tissue-Engineered Skeletal Muscle: A Tool for Metabolic Research. *Endocrinol Metab* **37**, 408–414 (2022).

25. Dennis, R. G. & Kosnik, Ii, P. E. EXCITABILITY AND ISOMETRIC CONTRACTILE PROPERTIES OF MAMMALIAN SKELETAL MUSCLE CONSTRUCTS ENGINEERED IN VITRO. *In Vitro Cell Dev Biol Anim* **36**, 327 (2000).

26. Ebrahimi, M. *et al.* De novo revertant fiber formation and therapy testing in a 3D culture model of Duchenne muscular dystrophy skeletal muscle. *Acta Biomaterialia* **132**, 227–244 (2021).

27. Dessauge, F., Schleder, C., Perruchot, M.-H. & Rouger, K. 3D in vitro models of skeletal muscle: myopshere, myobundle and bioprinted muscle construct. *Vet Res* **52**, 72 (2021).

28. Carraro, E., Rossi, L., Maghin, E., Canton, M. & Piccoli, M. 3D in vitro Models of Pathological Skeletal Muscle: Which Cells and Scaffolds to Elect? *Front. Bioeng. Biotechnol.* **10**, 941623 (2022).

29. Mankhong, S. *et al.* Experimental Models of Sarcopenia: Bridging Molecular Mechanism and Therapeutic Strategy. *Cells* **9**, 1385 (2020).

30. Giza, S. *et al.* Microphysiological system for studying contractile differences in young, active, and old, sedentary adult derived skeletal muscle cells. *Aging Cell* **21**, e13650 (2022).

31. Parafati, M., Thwin, Z., Malany, L. K., Coen, P. M. & Malany, S. Microgravity Accelerates Skeletal Muscle Degeneration: Functional and Transcriptomic Insights from a Muscle Lab-on-Chip Model Onboard the ISS. Preprint at https://doi.org/10.1101/2025.01.26.634580 (2025).

32. Pedrotty, D. M. *et al.* Engineering skeletal myoblasts: roles of three-dimensional culture and electrical stimulation. *American Journal of Physiology-Heart and Circulatory Physiology* **288**, H1620–H1626 (2005).

33. Huang, Y.-C., Dennis, R. G. & Baar, K. Cultured slow vs. fast skeletal muscle cells differ in physiology and responsiveness to stimulation. *American Journal of Physiology-Cell Physiology* **291**, C11–C17 (2006).

34. Flaibani, M. *et al.* Muscle Differentiation and Myotubes Alignment Is Influenced by Micropatterned Surfaces and Exogenous Electrical Stimulation. *Tissue Engineering Part A* **15**, 2447–2457 (2009).

35. Hurley, B. F., Hanson, E. D. & Sheaff, A. K. Strength Training as a Countermeasure to Aging Muscle and Chronic Disease: *Sports Medicine* **41**, 289–306 (2011).

36. Cruz-Jentoft, A. J. *et al.* Sarcopenia: revised European consensus on definition and diagnosis. *Age and Ageing* **48**, 16–31 (2019).

37. Dyle, M. C. *et al.* Systems-based Discovery of Tomatidine as a Natural Small Molecule Inhibitor of Skeletal Muscle Atrophy. *Journal of Biological Chemistry* **289**, 14913–14924 (2014).

38. Ebert, S. M. *et al.* Identification and Small Molecule Inhibition of an Activating Transcription Factor 4 (ATF4)-dependent Pathway to Age-related Skeletal Muscle Weakness and Atrophy. *Journal of Biological Chemistry* **290**, 25497–25511 (2015).

39. Chiu, F.-L. & Lin, J.-K. Tomatidine inhibits iNOS and COX-2 through suppression of NF-κB and JNK pathways in LPS-stimulated mouse macrophages. *FEBS Letters* **582**, 2407–2412 (2008).

40. Kuo, C.-Y. *et al.* Tomatidine Attenuates Airway Hyperresponsiveness and Inflammation by Suppressing Th2 Cytokines in a Mouse Model of Asthma. *Mediators of Inflammation* **2017**, 1–9 (2017).

41. Zhao, B., Zhou, B., Bao, L., Yang, Y. & Guo, K. Alpha-Tomatine Exhibits Anti-inflammatory Activity

in Lipopolysaccharide-Activated Macrophages. *Inflammation* **38**, 1769–1776 (2015).

42. Parafati, M. *et al.* Human skeletal muscle tissue chip autonomous payload reveals changes in fiber type and metabolic gene expression due to spaceflight. *npj Microgravity* **9**, 77 (2023).

43. Liberzon, A. *et al.* The Molecular Signatures Database Hallmark Gene Set Collection. *Cell Systems* **1**, 417–425 (2015).

44. Moresi, V., Adamo, S. & Berghella, L. The JAK/STAT Pathway in Skeletal Muscle Pathophysiology. *Front. Physiol.* **10**, 500 (2019).

45. Hindi, L., McMillan, J., Afroze, D., Hindi, S. & Kumar, A. Isolation, Culturing, and Differentiation of Primary Myoblasts from Skeletal Muscle of Adult Mice. *BIO-PROTOCOL* **7**, (2017).

46. Yamawaki, Y., Kimura, H., Hosoi, T. & Ozawa, K. MyD88 plays a key role in LPS-induced Stat3 activation in the hypothalamus. *American Journal of Physiology-Regulatory, Integrative and Comparative Physiology* **298**, R403–R410 (2010).

47. Peake, J. M., Neubauer, O., Della Gatta, P. A. & Nosaka, K. Muscle damage and inflammation during recovery from exercise. *Journal of Applied Physiology* **122**, 559–570 (2017).

48. Dessauge, F., Schleder, C., Perruchot, M.-H. & Rouger, K. 3D in vitro models of skeletal muscle: myopshere, myobundle and bioprinted muscle construct. *Vet Res* **52**, 72 (2021).

49. Nikolić, N. *et al.* Electrical Pulse Stimulation of Cultured Human Skeletal Muscle Cells as an In Vitro Model of Exercise. *PLoS ONE* **7**, e33203 (2012).

50. Saito, Y., Chikenji, T. S., Matsumura, T., Nakano, M. & Fujimiya, M. Exercise enhances skeletal muscle regeneration by promoting senescence in fibro-adipogenic progenitors. *Nat Commun* **11**, 889 (2020).

51. Khan, K. M. & Scott, A. Mechanotherapy: how physical therapists' prescription of exercise promotes tissue repair. *Br J Sports Med* **43**, 247–252 (2009).

52. Gleeson, M. *et al.* The anti-inflammatory effects of exercise: mechanisms and implications for the prevention and treatment of disease. *Nat Rev Immunol* **11**, 607–615 (2011).

53. Roubenoff, R. Physical Activity, Inflammation, and Muscle Loss. *Nutrition Reviews* **65**, S208–S212 (2008).

54. Scheffer, D. D. L. & Latini, A. Exercise-induced immune system response: Anti-inflammatory status on peripheral and central organs. *Biochimica et Biophysica Acta (BBA) - Molecular Basis of Disease* **1866**, 165823 (2020).

55. Latroche, C. *et al.* Coupling between Myogenesis and Angiogenesis during Skeletal Muscle Regeneration Is Stimulated by Restorative Macrophages. *Stem Cell Reports* **9**, 2018–2033 (2017).

56. Ross, M., Kargl, C. K., Ferguson, R., Gavin, T. P. & Hellsten, Y. Exercise-induced skeletal muscle angiogenesis: impact of age, sex, angiocrines and cellular mediators. *Eur J Appl Physiol* **123**, 1415–1432 (2023).

57. Schnyder, S. & Handschin, C. Skeletal muscle as an endocrine organ: PGC-1α, myokines and exercise. *Bone* **80**, 115–125 (2015).

58. Catoire, M., Mensink, M., Kalkhoven, E., Schrauwen, P. & Kersten, S. Identification of human exercise-induced myokines using secretome analysis. *Physiological Genomics* **46**, 256–267 (2014).

59. Hjorth, M. *et al.* The effect of acute and long-term physical activity on extracellular matrix and serglycin in human skeletal muscle. *Physiol Rep* **3**, e12473 (2015).

60. Tidball, J. G. Regulation of muscle growth and regeneration by the immune system. *Nat Rev Immunol* **17**, 165–178 (2017).

61. Langston, P. K. & Mathis, D. Immunological regulation of skeletal muscle adaptation to exercise. *Cell Metabolism* **36**, 1175–1183 (2024).

62. Pérez-Baos, S. *et al.* Mediators and Patterns of Muscle Loss in Chronic Systemic Inflammation. *Front. Physiol.* **9**, 409 (2018).

63. Silva, K. A. S. *et al.* Inhibition of Stat3 Activation Suppresses Caspase-3 and the Ubiquitin-Proteasome System, Leading to Preservation of

Muscle Mass in Cancer Cachexia. *Journal of Biological Chemistry* **290**, 11177–11187 (2015).

64. Huang, Z. *et al.* Inhibition of IL-6/JAK/STAT3 pathway rescues denervation-induced skeletal muscle atrophy. *Ann Transl Med* **8**, 1681–1681 (2020).

65. Xu, M. *et al.* JAK inhibition alleviates the cellular senescence-associated secretory phenotype and frailty in old age. *Proc. Natl. Acad. Sci. U.S.A.* **112**, (2015).

66. Chen, Z., Li, B., Zhan, R.-Z., Rao, L. & Bursac, N. Exercise mimetics and JAK inhibition attenuate IFN-γ–induced wasting in engineered human skeletal muscle. *Sci. Adv.* **7**, eabd9502 (2021).

67. Zimmers, T. A., Fishel, M. L. & Bonetto, A. STAT3 in the systemic inflammation of cancer cachexia. *Seminars in Cell & Developmental Biology* **54**, 28–41 (2016).

68. Chen, X. & Li, Y. Role of matrix metalloproteinases in skeletal muscle: Migration, differentiation, regeneration and fibrosis. *Cell Adhesion & Migration* **3**, 337–341 (2009).

69. Sprenger, H. *et al.* Enhanced release of cytokines, interleukin-2 receptors, and neopterin after long-distance running. *Clinical Immunology and Immunopathology* **63**, 188–195 (1992).

70. Drenth, J. P. *et al.* Endurance run increases circulating IL-6 and IL-1ra but downregulates ex vivo TNF-alpha and IL-1 beta production. *Journal of Applied Physiology* **79**, 1497–1503 (1995).

71. Nehlsen-Cannarella, S. L. *et al.* Carbohydrate and the cytokine response to 2.5 h of running. *Journal of Applied Physiology* **82**, 1662–1667 (1997).

72. Begue, G. *et al.* Early Activation of Rat Skeletal Muscle IL-6/STAT1/STAT3 Dependent Gene Expression in Resistance Exercise Linked to Hypertrophy. *PLoS ONE* **8**, e57141 (2013).

73. Trenerry, M. K., Carey, K. A., Ward, A. C. & Cameron-Smith, D. STAT3 signaling is activated in human skeletal muscle following acute resistance exercise. *Journal of Applied Physiology* **102**, 1483–1489 (2007).